CIRSE

LABORATORY INVESTIGATION

IMAGING

CBCT-Based Image Guidance for Percutaneous Access: Electromagnetic Navigation Versus 3D Image Fusion with Fluoroscopy Versus Combination of Both Technologies—A Phantom Study

Vania Tacher[1,2,3] · Maxime Blain[1] · Edouard Hérin[1,2] · Manuel Vitellius[1] ·
Mélanie Chiaradia[1] · Nadia Oubaya[4,5] · Haytham Derbel[1,2,3] · Hicham Kobeiter[1,2]

Abstract

Purpose We set out to compare three types of three-dimensional CBCT-based imaging guidance modalities in a phantom study: image fusion with fluoroscopy (IF), electromagnetic navigation (EMN) and the association of both technologies (CEMNIF).

Materials and Methods Four targets with a median diameter of 11 mm [first quartile (Q1): 10; third quartile (Q3): 12] with acute angle access (z-axis $< 45°$) and four targets of 10 mm [8–15] with large angle access (z-axis $> 45°$) were defined on an abdominal phantom (CIRS, Meditest, Tabuteau, France). Acute angle access targets were punctured using IF, EMN or CEMNIF and large angle access targets with EMN by four operators with various experiences. Efficacy (target reached), accuracy (distance between needle tip and target center), procedure time, radiation exposure and reproducibility were explored and compared.

Results All targets were reached (100% efficacy) by all operators. For targets with acute angle access, procedure times (EMN: 265 s [236–360], IF: 292 s [260–345], CEMNIF: 320 s [240–333]) and accuracy (EMN: 3 mm [2–5], IF: 2 mm [1–3], CEMNIF: 3 mm [2–4]) were similar. Radiation exposure (EMN: 0; IF: 708 mGy.cm^2 [599–1128]; CEMNIF: 51 mGy.cm^2 [15–150]; $p < 0.001$) was significantly higher with IF than with CEMNIF and EMN. For targets with large angle access, procedure times (EMN: 345 s [259–457], CEMNIF: 425 s [340–473]; $p = 0.01$) and radiation exposure (EMN: 0, CEMIF: 159 mGy.cm^2 [39–316]; $p < 0.001$) were significantly lower with EMN but with lower accuracy (EMN: 4 mm [4–6] and CEMNIF: 4 mm [3, 4]; $p = 0.01$). The operator's experience did not impact the tested parameters regardless of the technique.

Conclusion In this phantom study, EMN was not limited to acute angle targets. Efficacy and accuracy of puncture for acute angle access targets with EMN, IF or CEMNIF were similar. CEMNIF is more accurate for large angle access targets at the cost of a slightly higher procedure time and radiation exposure.

Keywords 3D image guidance · CBCT · Percutaneous intervention · Electromagnetic navigation · Phantom study · Radiation exposure · Accuracy

✉ Vania Tacher
vania.tacher@aphp.fr

1 Assistance Publique – Hôpitaux de Paris (AP-HP), Service d'Imagerie Médicale, CHU Henri Mondor, 51 Avenue du Maréchal de Lattre de Tassigny, 94010 Créteil, France

2 Université Paris-Est Créteil (UPEC), 94010 Créteil, France

3 Unité INSERM U955 #18, IMRB, Créteil, France

4 Service de santé publique, APHP Hôpital Henri Mondor, Créteil, France

5 UPEC, DHU A-TVB, IMRB-EA 7376 CEpiA (Clinical Epidemiology And Ageing Unit), Paris-Est University, 94000 Créteil, France

Introduction

Image guidance is at the center of interventional radiology. An operator can choose between various imaging modalities depending on the type of procedure and taking into account important parameters such as accuracy, patient accessibility, spatial and temporal resolutions and exposure to radiation. A major concern for both patient and operator is exposure to radiation because of both determinist and stochastic risks [1]. Ultrasound guidance is often chosen for a percutaneous approach of solid organs for its accuracy, spatial and temporal resolutions and radiation-free exposure [2]. Computed tomography (CT) is mainly used for organs containing air such as the lung or bowel or for deep targets like retroperitoneum lymph nodes [3, 4]. The main drawbacks of CT are that it involves radiation exposure and that the target angle access is limited to 30 degrees (°) in a z-axis (i.e., table axis) [5]. Cone-beam computed tomography (CBCT) provides 3D "CT-like" images and image fusion imaging in the interventional radiology suite [6]. It enables 3D image guidance for multiple interventions whether they be endovascular or percutaneous [7, 8]. Image guidance using image fusion has transformed routine practice by overlaying any 3D pre-intervention diagnostic imaging or pre-intervention CBCT images onto 2D live fluoroscopy [9–11]. It is becoming increasingly used especially for trans-arterial chemoembolization and endovascular aortic repair [12–16]. For percutaneous interventions, CBCT allows 3D image guidance for an angle access up to 45° in the z-axis for percutaneous puncture with an ablation efficiency comparable to that of CT scan [8, 17].

The electromagnetic guidance system IMACTIS-CT® (La Tronche, France) enables the radiologist to explore the patient's anatomy, visualize the planned needle path and track needle position. Its association with CT for thoraco-abdominal percutaneous access showed higher accuracy with similar procedure time and radiation exposure compared with CT guidance alone in a clinical trial [18, 19].

The primary aim of this phantom study was to compare the efficacy of CBCT-based images with electromagnetic navigation (EMN), image fusion onto 2D live fluoroscopy (IF) or the combination of both technologies (CEMNIF) in a percutaneous approach. The secondary objectives were to assess accuracy, procedure time, radiation exposure and inter-observer reproducibility. We compared EMN, IF and CEMNIF guidance for targets with acute angle access (z-axis < 45°), and EMN and CEMNIF for large angle access (z-axis > 45°).

Materials and Methods

This study was performed between December 2017 and March 2018. All experiments were performed in the same angiography suite equipped with a CBCT C-arm with a flat-panel detector (Philips FD20, Philips Healthcare, Best, The Netherlands).

Phantom and Defined Targets

This study used a 28 × 20 × 12.5 cm abdominal phantom with a total of 12 possible targets from 5 to 12 mm in diameter (Model 071B CIRS, Norfolk, VA) (Fig. 1). The phantom was placed on the table of the angiography suite, blocked with two sandbags to avoid any movement and covered with a drape for all procedures.

For each target, an entry point was defined and provided to the operator to vary angulations and depths. A total of eight targets were used for this study. Four targets had acute angle access (z-axis < 45°) and were numbered from 1 to 4 (Fig. 1A), with a median diameter of 11 mm [first quartile (Q1): 10, third quartile (Q3): 12]. Four targets had large angle access (> 45°) and were numbered from 5 to 8 (Fig. 1B) with a median diameter of 10 mm [Q1: 8–Q3: 15].

A threshold angle of 45° on the z-axis (i.e., table axis) was defined because beyond 45° the C-arm collided with the angiography table thus restricting the entry point angle when using image fusion (IF) guidance as described.

Puncture Sessions

All the targets were punctured in separate sessions by four operators with various experiences in interventional radiology [operators 1 (AA), 2 (BB), 3 (CC) and 4 (DD) with 20, 8, 6 and 3 years' experience, respectively]. Each operator successively punctured all the pre-defined targets and trajectories in the same order (1–4 for acute angle access and 5–8 for large angle access) using the same 18 cm 20 G Chiba biopsy needle (Cook medical, Bloomington, IN). Different sessions were necessary using the three image guidance modalities consecutively to minimize the learning experience in data collection.

CBCT Scan Acquisition

An unenhanced CBCT scan was systematically performed for each of the three image guidance modalities pre-puncture for planning and targeting, and then post-puncture to assess efficacy (whether the target was reached or not) and accuracy (distance between the needle tip and the target center) (Fig. 2). The area of interest was positioned

Fig. 1 3D reconstructed views with a volume rendering technique of the phantom and its targets. The eight targets used for the study are numbered from 1 to 8. The paths to reach the targets with acute angles (targets 1–4) are represented on **A** and with large angles (targets 4–8) on **B**
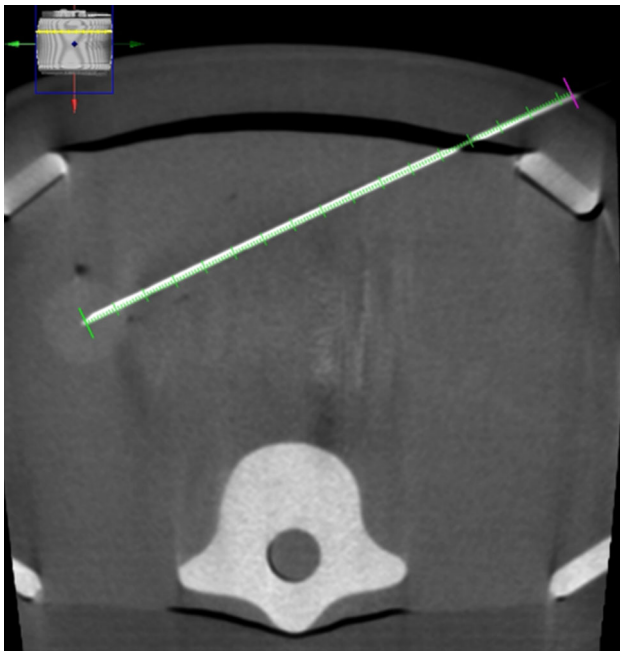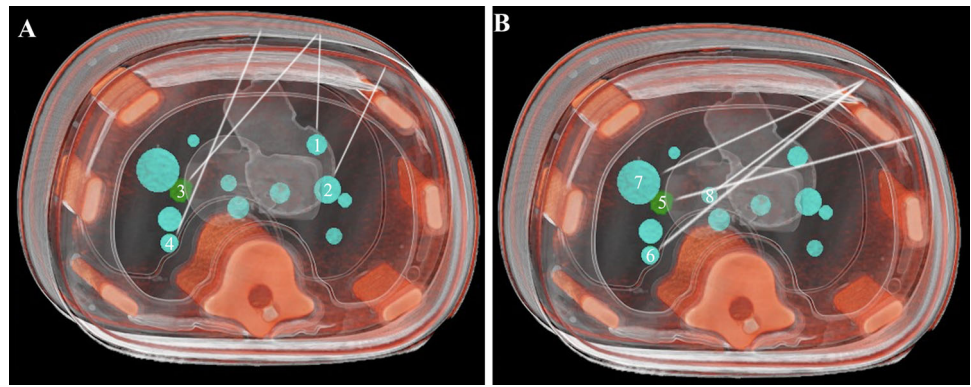
Fig. 2 Coronal view of a monitor CBCT image of the needle tip position in target 7 with IF. The needle perfectly follows the path on the progress view image. The CBCT monitoring confirms the excellent accuracy (distance between the center of the target and the needle tip: 0 mm)

in the system's isocenter, and 120 projections (15 frames per second) were acquired over a 180° arc (120 kV; 76 mAs; matrix diameter: 512 × 512; field of view 25 × 25 × 19 cm). The images were reconstructed into a 3D volume (XperCT, Philips Healthcare, Best, The Netherlands) on the workstation (Xtravision Release 8, Philips Healthcare).

Electromagnetic Navigation (EMN)

EMN image guidance was performed with an EMN system for CT-guided interventional radiological procedures called Imactis-CT® (La Tronche, France). Imactis obtained

CE marking as a medical device in 2013 and is composed of the following components (Fig. 3A):

1. A navigation station including a computer, a touch screen, an electromagnetic transmitter attached to the phantom and an electromagnetic receiver attached to the needle holder (Fig. 3).
2. Navigation software that has been specifically designed for CBCT-guided percutaneous interventions.
3. Hardware that contains the software parameters and which enables the software to be launched.

The operating principle of the navigation system is based on the localization (position and orientation) in real time of the needle holder, equipped with an electromagnetic receiver, with respect to the phantom by means of the electromagnetic transmitter that is attached to the phantom's surface. A registration process enables a previously acquired CBCT scan of the phantom to be positioned in the CBCT field of view. The operator can then visualize the position of the instrument on the CBCT images. Therefore, during the planning phase, the hypothetical needle path, calculated from the current position of the needle holder, can be visualized to determine the optimal route before surface penetration. During the needle insertion phase of the procedure, the operator visualizes the progression of the needle through the phantom (Fig. 3B and C) as the electromagnetic receiver at the bottom of the needle slides along to display the needle tip position. All participating operators had previously been trained on the system in two separate sessions.

Image Fusion onto 2D Live Fluoroscopy Guidance

All CBCT images were viewed on a dedicated 3D workstation (Xtra Vision Release 8; Philips Healthcare) to plan the 3D puncture path: entry point and progress views to the target as previously described using dedicated software (Xperguide, Philips Healthcare) [10, 20].
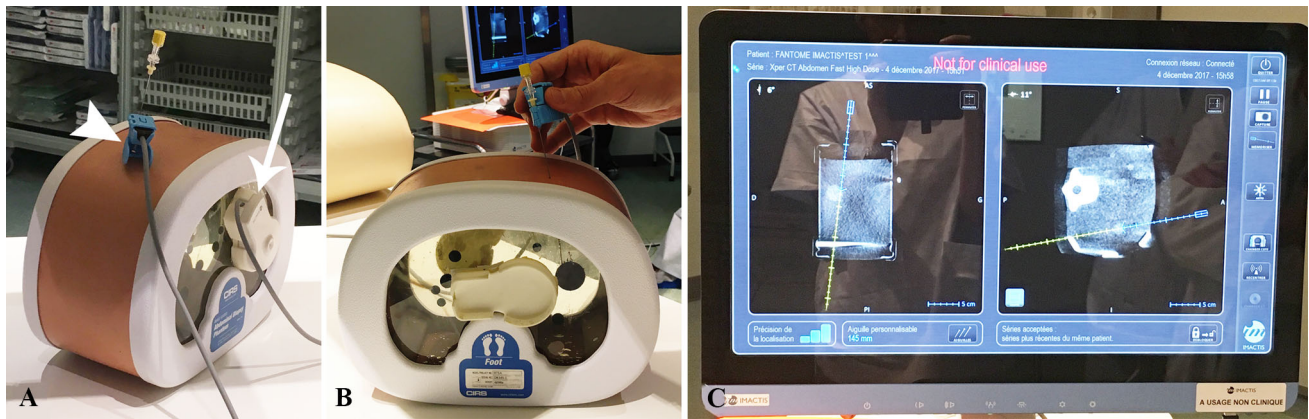
Fig. 3 Pictures of the phantom and the navigation station screen taken during teaching experience and used for the study. **A** The detector is placed on the phantom in the field of view for CBCT image acquisition (arrow). The needle is guided with the electromagnetic receiver (arrowhead). **B** The operator slices the emitter on the needle bottom to determine the needle tip position as indicated on the screen. The screen (**C**) displays that target 7 was reached according to the two (sagittal and coronal) views of CBCT images, the needle path (yellow line) and the needle tip position (blue arrow)

The image fusion process enabled an overlay of the 3D needle path onto live 2D-fluoroscopy. The optimal C-arm angulation for the two orthogonal views during puncture (entry point) and needle progression (progression view) were saved and used accordingly (Fig. 4). The generated 3D puncture path was synchronized with the C-arm/table positions to provide a live update and match the 2D fluoroscopy at any C-arm/table angle, position and magnification.

Combination of Electromagnetic Navigation and Image Fusion onto 2D Live Fluoroscopy Guidance (CEMNIF)

All images were viewed on a dedicated 3D workstation (Xtra Vision Release 8; Philips Healthcare) to plan the puncture path: entry point and progress views to the defined target. The image fusion process helped determine the needle path and the optimal orthogonal C-arm angulation for the needle trajectory.

For acute angle access, the operator visualized the position of the puncture site with both modalities: IF and EMN. Needle progression was then mainly monitored with IF.

For large angle access, the operator visualized the position of the needle insertion with EMN and needle progression was then monitored with IF and EMN.

Data Analysis

Each operator punctured a total of eight targets in various sessions: four with acute angle access using each of the three imaging modalities (EMN, IF, CEMNIF) and four

Fig. 4 Example of entry point (**A**) and progress (**B**) views of the puncture of target 4 with IF. The 3D needle path in green was overlaid on the 2D fluoroscopy. The target was reached. The center of the purple round landmark displays the entry point, whereas the center of the green round landmark indicates the center of the target
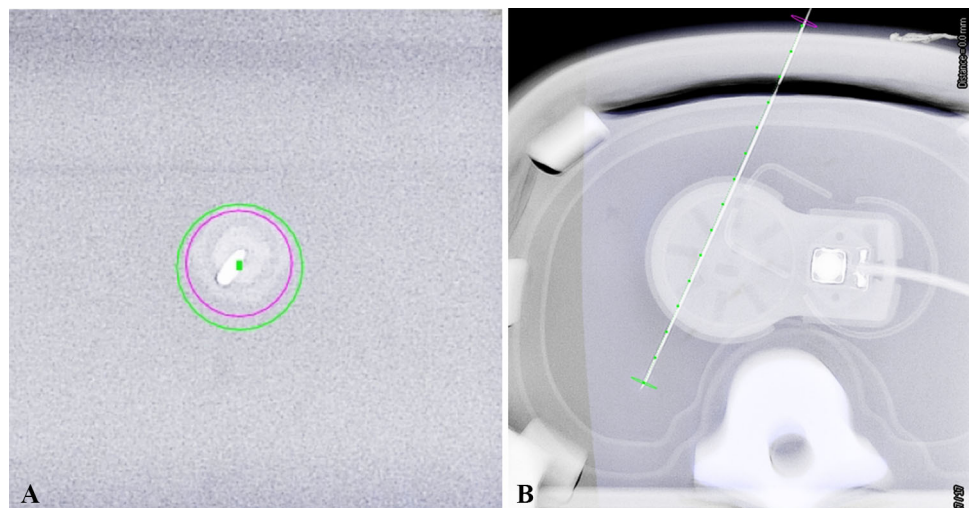
targets with large angle access on two imaging modalities (EMN, CEMNIF).

The primary endpoint was the efficacy of the image guidance technique (whether the target was reached or not). The secondary endpoints were as follows: (A) accuracy: distance in millimeters between the tip of the needle and the center of the target measured from the post-puncture CBCT on the workstation (Release 8.8, Philips Healthcare); (B) the distance of the needle trajectory into the phantom (distance between the tip of the needle and the phantom surface). (C) planning time (time from the end of CBCT acquisition to the start of the puncture); (D) puncture time (time from the start of the puncture until the target was reached) and then, (E) total procedure time (the sum of planning and puncture times), (F) radiation exposure, represented by dose area product (DAP in mGy*cm^2) and (G) fluoroscopy time (seconds: s).

Statistical Analysis

Because all variables were not normally distributed according to the Shapiro test, the continuous variables were represented as median and first and third quartiles [Q1–Q3] and non-continuous variables as sums and percentages. Comparisons between imaging modalities were done with the Kruskal–Wallis test for continuous variables. In the case of statistically significant differences, further comparisons between imaging modalities were performed by Wilcoxon tests (experiment-wise error rate of 0.05) for pairwise comparisons between imaging modalities. The same tests were performed to assess differences in performance between operators. A two-sided p value less than 0.05 was considered statistically significant. Statistical analysis was performed with R (R studio, Version 1.0.143, Boston, MA).

Results

All the operators reached all the targets with all the image guidance modalities regardless of angle access and operator experience. The results are reported in Table 1 and Fig. 5 for acute angle access and Fig. 6 for large angle access.

For Targets with Acute Angle Access

The planning times (EMN: 69 s [60–76]; IF: 105 s [60–123]; CEMNIF: 135 s [120–155]) were significantly different ($p < 0.001$) and lower with EMN. Puncture times were similar with all image guidance modalities (EMN: 205 s [180–250]; IF: 205 s [168–250]; CEMNIF: 150 s [113–203]; $p = 0.06$) as were total procedure times (265 s

[236–360], 292 s [260–345], 320 s [240–333], respectively; $p = 0.76$).

Radiation exposure (DAP) was significantly lower with EMN (EMN: 0; IF: 708 mGy.cm^2 [599–1128], CEMNIF: 51 mGy.cm^2 [15–150]; $p < 0.001$) as were fluoroscopy times (0 s, 65 s [57–96] and 6 s [1–21], respectively; $p < 0.001$).

Accuracy was similar for all three imaging modalities (EMN: 3 mm [2–5]; IF: 2 mm [1–3] and; CEMNIF: 3 mm [2–4]; $p = 0.08$).

No difference in total procedure time or accuracy was found according to the operators for any of the imaging modalities (Fig. 6). Operator 1 (the most senior operator) used significantly more radiation with IF than operator 2 ($p = 0.03$). Operator 1 also used significantly more radiation with CEMNIF than the other three operators ($p = 0.03$).

For Targets with Large Angle Access

The total procedure times were lower with EMN compared with CEMNIF (345 s [259–457] and 425 s [340–473], respectively; $p = 0.01$). The planning times were also significantly lower with EMN (93 s [60–125] and 155 s [148–180], respectively; $p = 0.004$). Nevertheless, the puncture times were similar (249 s [165–338] and 260 s [205–308], respectively; $p = 0.75$).

No radiation was required with EMN (EMN: 0 and CEMNIF: 159 mGy.cm^2 [39–316], $p < 0.001$). No fluoroscopy time was required for EMN either (EMN: 0 and CEMNIF: 13 s [7–25], $p < 0.001$).

Accuracy was significantly higher with CEMNIF (EMN: 4 mm [4–6] and CEMNIF: 4 mm [3, 4], $p = 0.01$).

No differences were found according to the operator for any of the study parameters regardless of the imaging modality used (Fig. 7).

Discussion

This phantom study was the first to combine two recent technologies based on CBCT images: IF and EMN. The main findings were that CBCT image-based guidance with EMN, IF and CEMNIF are effective and accurate in reaching targets with acute angle access. Furthermore, EMN, unlike IF guidance, could reach targets with large angle access in our model. The combination of both image guidance types—CEMNIF—significantly increased accuracy especially for targets with large angle access at the cost of slightly higher radiation exposure and total procedure time regardless of the operator's experience.

To the best of the authors' knowledge, this is the first study to take into account various target angle accesses for

Table 1 Study parameters according to target angle access and image guidance modality

| Image guidance modality	EMN Median [Q1–Q3]	IF Median [Q1–Q3]	CEMNIF Median [Q1–Q3]	p value
Targets with acute angle access (< 45°)				
Target diameter (mm)	11 [10–12]	11 [10–12]	11 [10–12]	–
Depth (mm)	98 [92–135]	109 [87–129]	99 [87–133]	0.95
Total time (s)	265 [236–360]	292 [260–345]	320 [240–333]	0.76
Planification time (s)	69 [60–76]	105 [60–123]	135 [120–155]	< 0.0001
Puncture time (s)	205 [180–250]	205 [168–250]	150 [113–203]	0.06
DAP (mGy × cm^2)	0	708 [599–1128]	51 [15–150]	< 0.0001
Fluoroscopy time (s)	0	65 [57–96]	6 [1–21]	< 0.0001
Accuracy (mm)	3 [2–5]	2 [1–3]	3 [2–4]	0.08
Targets with large angle access (> 45°)				
Target diameter (mm)	10 [8–15]	–	10 [8–15]	–
Depth (mm)	168 [156–169]		169 [146–172]	0.56
Total time (s)	345 [259–457]		425 [340–473]	0.01
Planification time (s)	93 [60–125]		155 [148–180]	0.004
Puncture time (s)	249 [165–338]		260 [205–308]	0.75
DAP (mGy × cm^2)	0		159 [39–316]	< 0.0001
Fluoroscopy time (s)	0		13 [7–25]	< 0.0001
Accuracy (mm)	4 [4–6]		4 [3–4]	0.01

CBCT cone-beam computed tomography, *DAP* dose area product, *mm* millimeter, *s* seconds, *Q1* first quartile, *Q3* third quartile
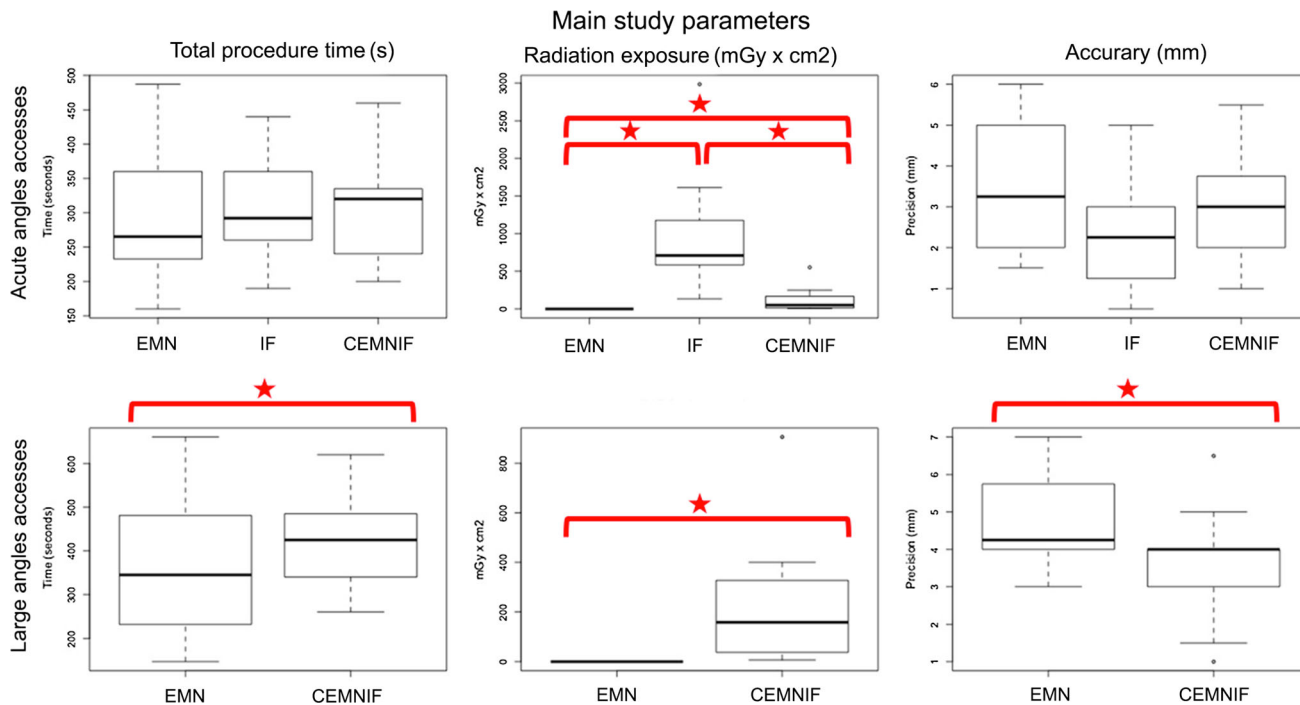
Fig. 5 Graphs of the main study parameters: total procedure time, x-ray exposure and accuracy according to the target angle access and the image modality used. The red stars indicate statistically significant differences. DAP: Dose area product

percutaneous approach based on CBCT images and highlights the trend toward multimodality image fusion to widen the scope of application [7]. The interventional radiologist is becoming increasingly reliant on multimodality image guidance while constantly being aware of
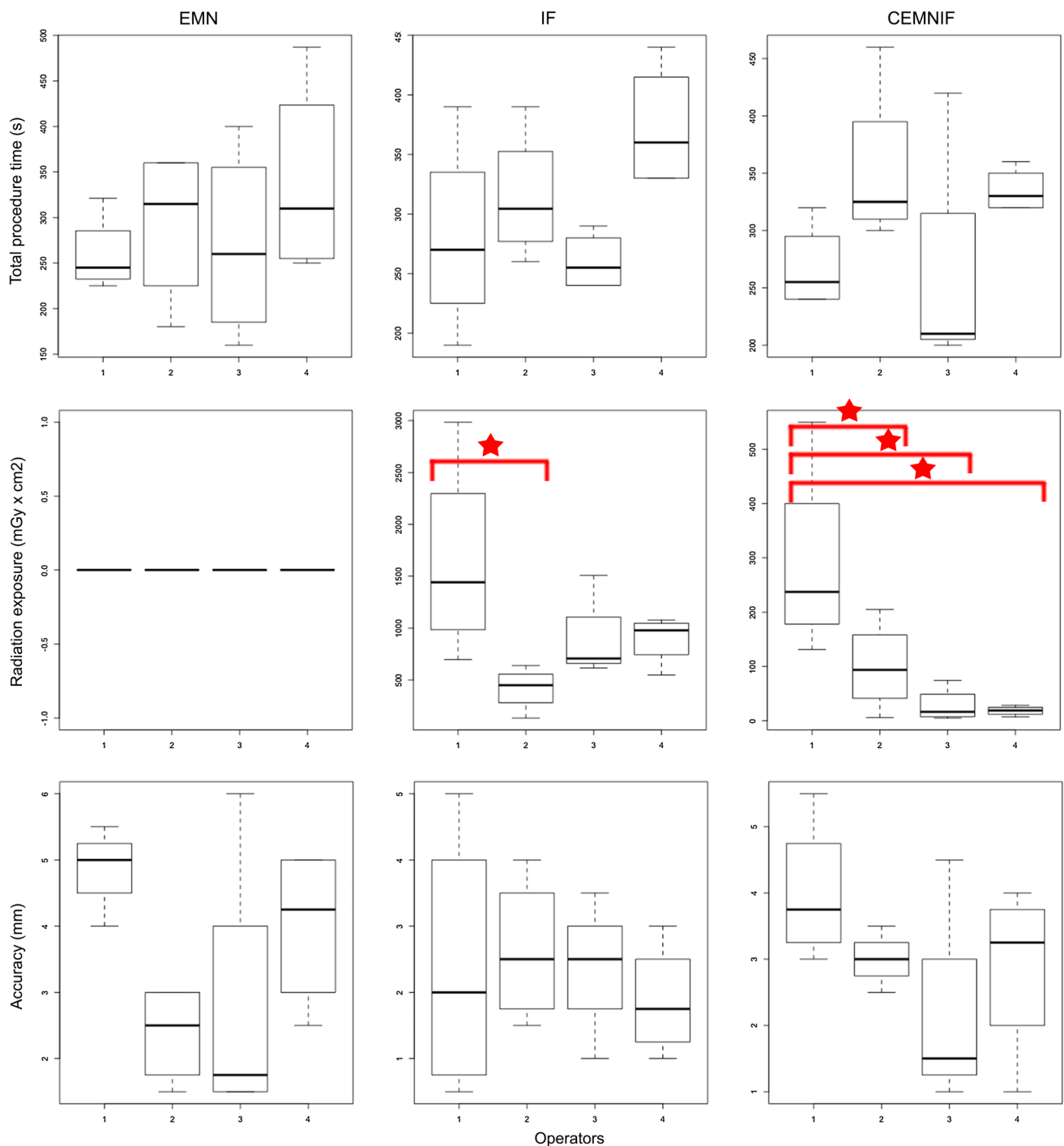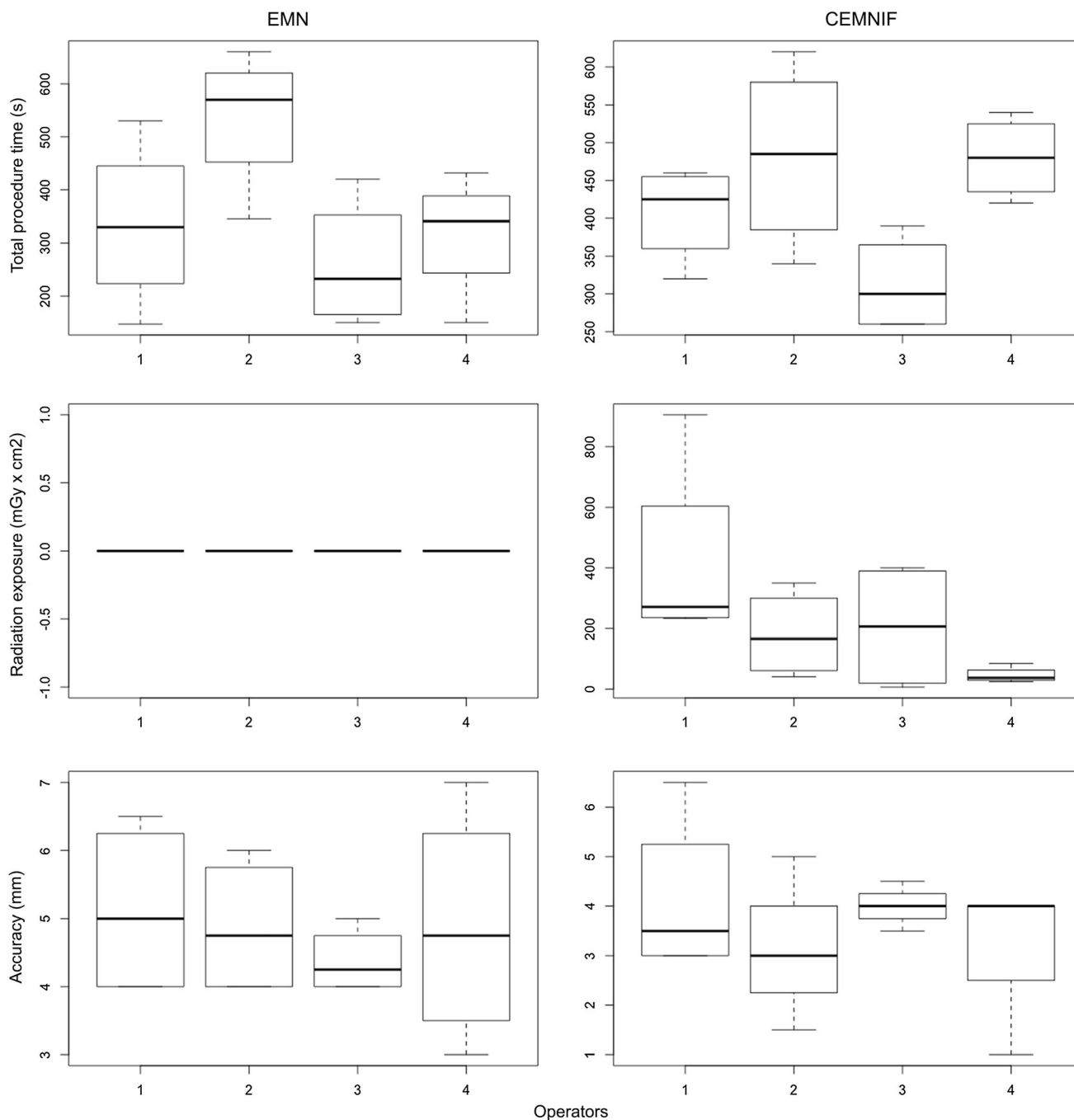
Fig. 6 Graphs of the main study parameters: total procedure time, x-ray exposure and accuracy according to the operator and the image modality used for targets with acute angle access. The red stars indicate statistically significant differences between operators. DAP: Dose area product

the need to limit procedure time and radiation exposure and obtain maximum accuracy.

One limitation of the EMN is that accuracy may be impaired by the needle bending (voluntary bending performed by experienced operators for needle path adjustment or needle deformation induced by the different nature of the tissues crossed). This does not occur with image fusion guidance because of live visibility of the needle. This may explain the difference in accuracy for targets with large angle access in our study between EMN and CEM-NIF guidance. Moreover, with EMN, operators have to follow the needle path simultaneously on one screen split in two orthogonal views, which could be challenging. Furthermore, the depth of the needle is not provided as a

Fig. 7 Graphs of the main study parameters: total procedure time, x-ray exposure and accuracy according to the operator and the image modality used for targets with large angle access. DAP: Dose area product

real time progression. Nevertheless, the need to evaluate the needle position did not impair the median total procedure time or the median puncture time compared to the IF modality.

One drawback of IF guidance is that the entry point angle is limited to 45° on the z-axis. This can be overcome by combining it with EMN (i.e., CEMNIF) as reported in our study. Moreover, IF guidance imposes multiple C-arm

replacements between the two views (entry and progress points views), which are time consuming for needle progression. Nevertheless, this did not impair the median total procedure or puncture times compared with EMN.

There were no differences in total procedure time, radiation exposure or accuracy between operators with various experience levels either according to the imaging modality or the target angle access confirming excellent

reproducibility. For targets with acute angle access, the most senior operator tended to use more radiation than the less-experienced operator 2 with IF guidance, and than the other operators when using the combination of both technologies. These differences were not found for targets with large angle access. This could be explained by the different habits of the senior operator.

Multimodality imaging of EMN with CBCT image-based guidance enables fluoroscopy images, image fusion of pre-intervention imaging onto live fluoroscopy as well as easier patient accessibility (C-arm with large trajectory position versus CT gantry [21]) compared with EMN with CT images.

Other guidance systems, such as augmented reality video assisted guidance with CBCT images that reduces radiation exposure during the puncture access, have also been developed [22].

The limitations of this study are as follows. (A) We do not report the number of times the needle was repositioned because of its subjective nature due to partial or complete repositioning possibilities. In contrast, fluoroscopy and total puncture times were objective criteria that could be collected. (B) The use of a phantom provides easily visible targets on CBCT images with a median depth of 11 cm, but this does not necessarily represent real life clinical conditions. Moreover, the accuracy may be impaired with deeper targets and various surrounding tissues. (C) The absence of phantom movement means that our results could be more promising than in real life as movement could induce the need of multiple CBCT acquisitions and additional use of radiation. (D) The radiation exposure during the pre- and post-CBCT procedures was not taken into account because we focused on image guidance parameters. However, these acquisitions were similar for all image guidance modalities.

Conclusion

The efficacy, accuracy and procedure time of target puncture with acute angle access are similar with EMN, IF and CEMNIF image guidance modalities. The advantage of EMN is that it does not require radiation to reach the target and it is not limited by target angle access unlike IF guidance. The efficacy of EMN and CEMNIF image guidance for large target angle access is similar with the CEMNIF image modality increasing accuracy at the cost of a slight increase in radiation exposure and procedure time. All the punctures were reproducible among operators of various experiences with similar total procedure time, radiation exposure and accuracy regardless of target angle access. EMN is a promising technology enabling large angle access and significant reduction or suppression of radiation exposure with an excellent accuracy. These results need to be confirmed in a clinical trial. Nevertheless, it is very likely that, in the near future, all these technologies will be integrated in the same angiography suite to facilitate and optimize the use of multimodality image guidance with a customized monitoring.

References

1. Little MP, Wakeford R, Tawn EJ, Bouffler SD, Berrington de Gonzalez A. Risks associated with low doses and low dose rates of ionizing radiation: why linearity may be (almost) the best we can do. Radiology. 2009;251:6–12.
2. Fenster A, Bax J, Neshat H, Cool D, Kakani N, Romagnoli C. 3D ultrasound imaging in image-guided intervention. In: Conference proceedings: annual international conference of the IEEE engineering in medicine and biology society IEEE engineering in medicine and biology society conference. 2014, vol. 2014, p. 6151–6154
3. Khankan AA, Al-Muaikeel M. Image-guided percutaneous transthoracic biopsy in lung cancer: emphasis on CT-guided technique. J Infect Public Health. 2012;5(Suppl 1):S22–30.
4. Gupta S, Nguyen HL, Morello FA Jr, Ahrar K, Wallace MJ, Madoff DC, et al. Various approaches for CT-guided percutaneous biopsy of deep pelvic lesions: anatomic and technical considerations. Radiographics: Rev Publ Radiol Soc N Am, Inc. 2004;24:175–89.
5. Stern EJ, Webb WR, Gamsu G. CT gantry tilt: utility in transthoracic fine-needle aspiration biopsy. Work in progress. Radiology. 1993;187:873–4.
6. Tacher V, Radaelli A, Lin M, Geschwind JF. How I do it: cone-beam CT during transarterial chemoembolization for liver cancer. Radiology. 2015;274:320–34.
7. Abi-Jaoudeh N, Kruecker J, Kadoury S, Kobeiter H, Venkatesan AM, Levy E, et al. Multimodality image fusion-guided procedures: technique, accuracy, and applications. Cardiovasc Intervent Radiol. 2012;35:986–98.
8. Abi-Jaoudeh N, Fisher T, Jacobus J, Skopec M, Radaelli A, Van Der Bom IM, et al. Prospective randomized trial for image-guided biopsy using cone-beam CT navigation compared with conventional CT. J Vasc Interv Radiol JVIR. 2016;27:1342–9.
9. Tacher V, Desgranges P, You K, Ridouani F, Marzelle J, Kobeiter H. Feasibility of three-dimensional MR angiography image fusion guidance for endovascular abdominal aortic aneurysm repair. J Vasc Interv Radiol JVIR. 2016;27:188–93.
10. Tacher V, Petit A, Derbel H, Novelli L, Vitellius M, Ridouani F, et al. Three-dimensional image fusion guidance for transjugular intrahepatic portosystemic shunt placement. Cardiovasc Intervent Radiol. 2017;40:1732–9.
11. Deschamps F, Solomon SB, Thornton RH, Rao P, Hakime A, Kuoch V, et al. Computed analysis of three-dimensional cone-

beam computed tomography angiography for determination of tumor-feeding vessels during chemoembolization of liver tumor: a pilot study. Cardiovasc Intervent Radiol. 2010;33:1235–42.

12. Lucatelli P, Argiro R, Bascetta S, Saba L, Catalano C, Bezzi M, et al. Single injection dual phase CBCT technique ameliorates results of trans-arterial chemoembolization for hepatocellular cancer. Transl Gastroenterol Hepatol. 2017;2:83.

13. Lucatelli P, Argiro R, Ginanni Corradini S, Saba L, Cirelli C, Fanelli F, et al. Comparison of image quality and diagnostic performance of cone-beam CT during drug-eluting embolic transarterial chemoembolization and multidetector CT in the detection of hepatocellular carcinoma. J Vasc Interv Radiol JVIR. 2017;28:978–86.

14. Lucatelli P, Corona M, Argiro R, Anzidei M, Vallati G, Fanelli F, et al. Impact of 3D rotational angiography on liver embolization procedures: review of technique and applications. Cardiovasc Intervent Radiol. 2015;38:523–35.

15. Leger T, Tacher V, Majewski M, Touma J, Desgranges P, Kobeiter H. Image fusion guidance for in situ laser fenestration of aortic stent graft for endovascular repair of complex aortic aneurysm: feasibility, efficacy and overall functional success. Cardiovasc Intervent Radiol. 2019;42:1371–79.

16. Touma J, Kobeiter H, Majewski M, Tacher V, Desgranges P. Triple in situ antegrade laser fenestration of aortic stent-graft extension using fusion imaging for urgent treatment of symptomatic abdominal aneurysm with type 1 endoleak. Cardiovasc Intervent Radiol. 2018;41:513–7.

17. Abi-Jaoudeh N, Kobeiter H, Xu S, Wood BJ. Image fusion during vascular and nonvascular image-guided procedures. Tech Vasc Interv Radiol. 2013;16:168–76.

18. Rouchy RC, Moreau-Gaudry A, Chipon E, Aubry S, Pazart L, Lapuyade B, et al. Evaluation of the clinical benefit of an electromagnetic navigation system for CT-guided interventional radiology procedures in the thoraco-abdominal region compared with conventional CT guidance (CTNAV II): study protocol for a randomised controlled trial. Trials. 2017;18:306.

19. Durand P, Moreau-Gaudry A, Silvent AS, Frandon J, Chipon E, Medici M, et al. Computer assisted electromagnetic navigation improves accuracy in computed tomography guided interventions: a prospective randomized clinical trial. PLoS ONE. 2017;12:e0173751.

20. Tacher V, Lin M, Desgranges P, Deux JF, Grunhagen T, Becquemin JP, et al. Image guidance for endovascular repair of complex aortic aneurysms: comparison of two-dimensional and three-dimensional angiography and image fusion. J Vasc Interv Radiol JVIR. 2013;24:1698–706.

21. Schernthaner RE, Chapiro J, Sahu S, Withagen P, Duran R, Sohn JH, et al. Feasibility of a modified cone-beam CT rotation trajectory to improve liver periphery visualization during transarterial chemoembolization. Radiology. 2015;277:833–41.

22. Racadio JM, Nachabe R, Homan R, Schierling R, Racadio JM, Babic D. Augmented reality on a C-arm system: a preclinical assessment for percutaneous needle localization. Radiology. 2016;281:249–55.